Meccanica (2025) 60:2033–2046
https://doi.org/10.1007/s11012-025-01954-y

RESEARCH

A new theory of the dynamical collapse of no-tension structures under sequences of pulses of horizontal acceleration

Simona Coccia · Mario Como

Received: 2 November 2024 / Accepted: 14 February 2025 / Published online: 25 March 2025

Abstract The paper presents the main lines of a new theory of the seismic dynamics of masonry structures in the context of the masonry Heyman model. The seismic action is represented by a sequence of horizontal acceleration pulses of rectangular shape, alternating in sign, of given intensity and wavelength. The central point of the proposed new theory is the definition of the way in which the dynamical collapse takes place, occurring during the motion of the no-tension structure, excited by the seismic shaking. Two new aspects play a fundamental role in this definition. The first is the configuration of zero strength, in which the potential energy of the weights reaches its maximum and where the structure has completely lost its strength. The second is the occurrence of the gradual accumulation of deformation of the structure that takes place under the pulse sequence, in spite of the alternating pulse action. Collapse thus takes place under the simultaneous achievement of the configuration of zero strength and the arrival of the acceleration pulse that pushes the structure to go beyond this configuration. By increasing the pulse number of the sequence, collapse takes place under smaller values of horizontal acceleration intensity. Finally, an asymptotic sequence of pulses allows an equation to be formulated for the behaviour factor (the ratio of collapse horizontal acceleration intensity to the static acceleration) for safe seismic design.

Keywords Masonry · Rocking · Dynamic · Behavior factor

1 Introduction

The occurrence of a resonance condition between the seismic shaking and the oscillating structure is the greatest danger for a construction hit by an earthquake. The use of the response elastic spectrum (represented for example in Fig. 1) is at the base of this consideration.

The peak accelerations *PGA (later denoted with* A_0*)* of the real earthquakes are, on the other hand, too high to permit an anti-seismic design of structures in the elastic field. In this context, the attribution of the behaviour *q factor* is a realistic choice and implies a design at the elastic limit under the reduced peak ground acceleration A_0/q, entrusting the excess of the seismic action to the dissipative capacity of the structure. Numerous experimental and analytical studies for reinforced concrete and steel structures have been made to support the corresponding design prescriptions (an extensive literature review is reported in [1]).

This approach is also applied to masonry structures without any in-depth analysis. For example, in the Italian design rules [2], for the out-of-plane collapse

S. Coccia (✉) · M. Como
University of Rome "Tor Vergata", Via del Politecnico 1, 00133 Rome, Italy
e-mail: coccia@ing.uniroma2.it

check of masonry structures, $q=2$ is assumed. It is therefore easy to recognize that there is an inadequate underlying basis in the common approach to the seismic analysis of masonry structures.

There is nothing of elastic about the behaviour of masonry structures: this aspect entails great consequences in their dynamic response. The masonry material has low tensile strength, for this reason, the column, resting on a friction plane, represents the arche-type of the masonry no-tension structures [3]. Its rocking, in fact, with his alternating detachments from its base, simulates the oscillating motion of masonry structures following one after the other the opening and the closing of cracks, occurring without energy dissipation (Fig. 2). During the rocking motion, an energy dissipation can be considered when and if the impact occurs [4]. An innovative model for the dissipation in masonry arches be found in [5]. Many authors study the rocking of masonry structures (see for example [6–11]).

The archetype of an elastic structure is the elastic oscillator, or the pendulum (Fig. 3). The motion of the masonry column is hyperbolic while the motion of the pendulum, or of the elastic oscillator, is harmonic: the closer is the column to the vertical, the higher is its recall moment. On the contrary, the closer is the pendulum to the vertical, the smaller is the stabilizing moment of its weight.

Furthermore, there is not a period of the oscillation for a masonry no-tension structure, as shown Fig. 4 that describes the oscillations of the column with semi-periods that gradually reduce one after the

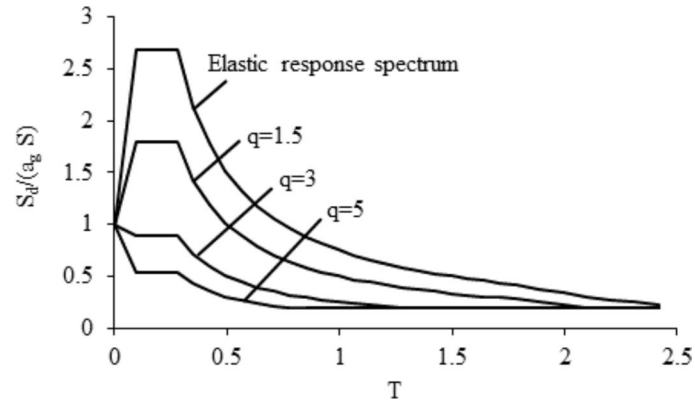

Fig. 1 The elastic and the elastic—plastic response spectra

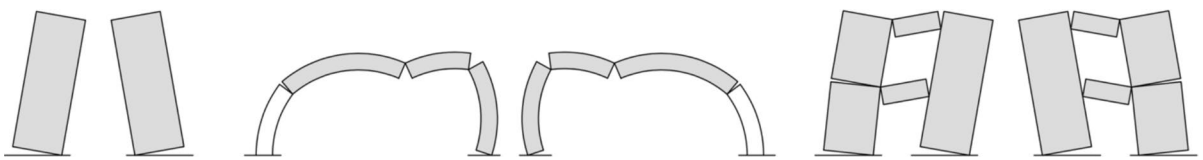

Fig. 2 Rocking of the column, of the masonry arch and of the masonry wall

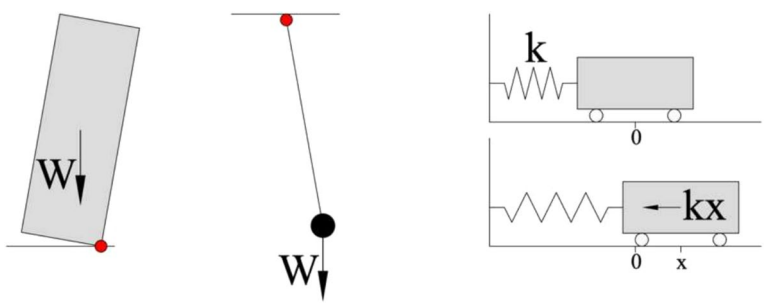

Fig. 3 Recall forces in the column, the pendulum and the elastic oscillator

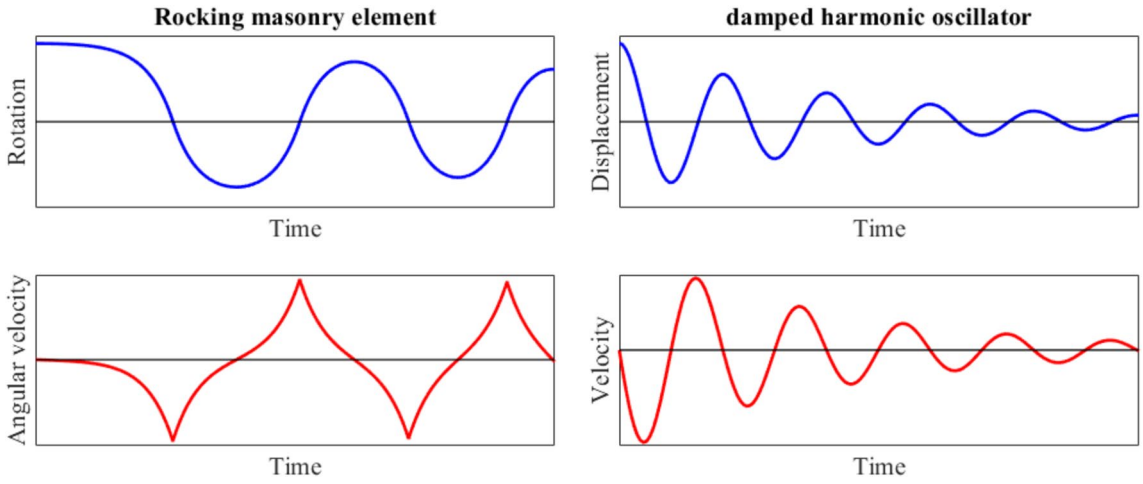

Fig. 4 Rocking of the column and motion of a damped harmonic oscillator

other, until the motion stop, in contrapposition with the motion of a damped harmonic oscillator.

We understand how far away is the real behaviour of masonry structures from that of the common model assumed in the current seismic design. In alternative to the model used for the elatic structures, this paper proposes a new approach for the seismic analysis of masonry structures. Direct reference in the paper is made to previous works of the authors [12–14] addressed to the specific dynamical behaviour of the column resting on a friction plane, and of the reinforced masonry wall or of the masonry arch, respectively under out of plane or in-plane seismic actions. Trying to fill the gaps with the common approach, the purpose of the paper is to give the main lines of the proposed new theory of the seismic collapse of no tension structures in the simplest way possible, in the full respect of the real behaviour of masonry structures and of the real nature of the seismic shaking, composed by a sequence of acceleration pulses alternating in sign, trying to fill the gaps with the common approach. The ultimate outcome of the proposed model is a formulation of the q factor that depends on both the seismic input and the geometric characteristics of the masonry structure to be analyzed.

The dynamical collapse of the no tension structure hit by a sequence of acceleration pulses alternating in sign presents completely different features from those that characterize the static collapse. When the static collapse takes place, the no tension structure only reaches that limit condition whereby it is no longer able to support the loads acting in a state of static equilibrium and must therefore start moving. Dynamic collapse instead develops, as shown below, when the moving structure reaches that particular configuration in which, at the same time, it has lost all resistance and the acting loads push it to go beyond this configuration. To better understand the particular features of the dynamic collapse, some recalls of static collapse are now made.

2 Recallecting the definition of the static collapse for no-tension structures

The masonry structures can be modelled as rigid bodies linked together by hinges without tensile strength and the impossibility of slindig failures. Generally, in addition to the dead load $\mathbf{w}$ (thereafter, lowercase letters will be used to represent distributed loads, and uppercase letters for concentrated forces), the live load $\mathbf{f}$ multiplied by a positive coefficient λ, also acts on the structure so that the overall load acting is:

$$\mathbf{q} = \mathbf{w} + \lambda \mathbf{f} \tag{1}$$

In the Limit Analisis context [15, 16], the structure is in an admissible equilibrium if the work of the load $\mathbf{q}$ is negative along each virtual compatible mechanism δu (Fig. 5):

$$< \mathbf{w}, \delta\mathbf{u} > + \lambda < \mathbf{f}, \delta\mathbf{u} > \leq 0 \, \forall \delta\mathbf{u} \in M \tag{2}$$

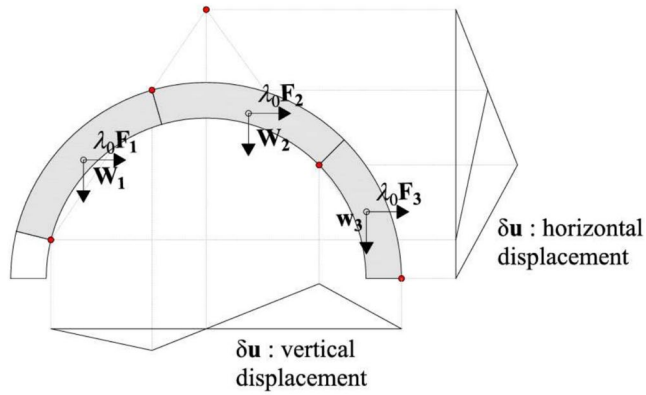

Fig. 5 Virtual displacement for which the live load **f** does positive work

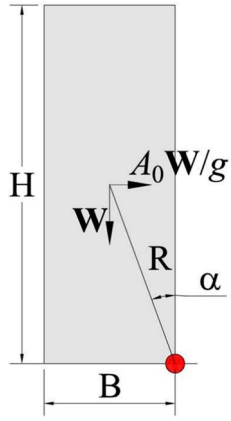

Fig. 6 The column at the limit of equilibrium hit by a static accelation pulse

where M is the class of kinematically admissible mechanisms for which the external load λf does positive work:

$$\lambda < \mathbf{f}, \delta \boldsymbol{u} >> 0 \, \forall \delta \boldsymbol{u} \in M \tag{3}$$

Displacements for which **f** does negative work cannot be considered for a collapse analysis of the structure.

Under a defined multiplier $\lambda = \lambda_0$, the load $\lambda_0\mathbf{f}$ can break the admissible equilibrium in the masonry structure along a definite mechanism $\mathbf{u}_0$ if:

$$< \mathbf{w}, \mathbf{u}_0 > + \lambda_0 < \mathbf{f}, \mathbf{u}_0 >= 0 \, \mathbf{u}_0 \in M \tag{4}$$

The statical collapse has taken place. Figure 6 shows the example of the column loaded by its own weight **W** and by the horizontal load $\lambda_0\mathbf{F} = \mathbf{W}A_0/g$ induced by a constant pulse of horizontal acceleration A_0 (g is the acceleration of gravity). The *static limit acceleration intensity* A_L, under which the column starts to move, is equal to g multiplied by the slenderness α of the element:

$$A_L = g\alpha\alpha = atan\left(\frac{B}{H}\right) \simeq \frac{B}{H} \tag{5}$$

or, equivalently:

$$\lambda_0 = \frac{A_L}{g} \tag{6}$$

that, for a generic no tension structure, is the load multiplier of the static distribution of loads representative of the pulse action. At the static collapse, by further increasing λ beyond λ_0, the structure puts itself in motion along the mechanism $\mathbf{u}_0$.

The dynamical collapse occurring under seismic action has instead completely different rules. To define them it is firstly necessary to schematize the seismic input.

3 Schematization of the seismic action

The common approach in the seismic design considers the seismic action as a particular static force or as a simple horizontal acceleration pulse. A typical seismic shaking is instead composed of a sequence of shocks made up of horizontal acceleration pulses that follow one after the other with different intensity. The most severe part of the accelerogram includes a more or less limited number of shocks of less irregular shape where the longest wavelength defines the period T_E of the earthquake (Fig. 7). More details about the procedure to evaluate T_E can be found in [12].

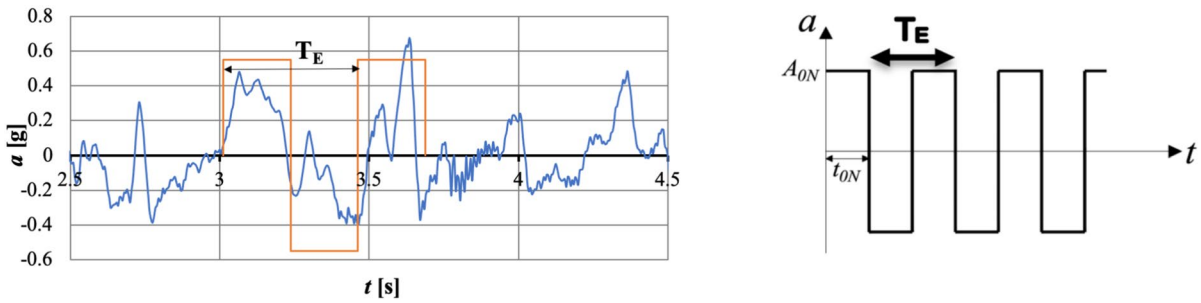

Fig. 7 Part of a real accelerogram and the idealized sequence of alternating pulses

In what follows the seismic shaking is assumed to consist of a sequence of alternating rectangular pulses of horizontal acceleration. In the proposed model, three quantities define the pulse sequence:

- The number N of pulses,
- The maximum acceleration A_{0N},
- The duration t_0 of the pulses, generally assum ed equal to $T_E/2$.

4 The configuration of zero strength

There is a particular configuration that can be crossed by the no-tension structure set in motion by the pulse sequence: *the configuration of zero strength*, later denoted by C_{ZS}. In this configuration, the potential energy of the weight forces reaches its maximum, and no deformation increment can be counteracted by the weight forces. For the column, the configuration of zero strength is defined by the rotation of the block until the reaching of value $\theta_{ZS}=\alpha\simeq$B/H (Fig. 8).

For no tension structures of more complex geometry, the motion is activated when internal hinges form and the structure (wall or arch for example) split into several rigid bodies (Figs. 2 and 8). In the proposed model, during the motion, until the configuration C_{ZS} is reached, hinge positions do not change, but they move in funtion of the rotation of the bodies (more details can be found in [13, 14]). The configuration C_{ZS} and the relatice rotation θ_{ZS} can be determined taking into account that the potential energy of the weights **W** reaches its maximum in it.

The motion of the structure starts at the configuration of the static collapse C_{SC}, mobilizing the mechanism $\mathbf{u}_0$. Finite deformations are present in the configuration of zero strength. Finite deformations will be therefore considered to describe the motion of the structure from the C_{SC} to the C_{ZS}. Consequentially, while the hinges of the mechanism $\mathbf{u}_0$ remain integral with the moving structure, it will be taken into account that the absolute centres of $\mathbf{u}_0$ change their position in the plane of the mechanism until the C_{ZS} is reached.

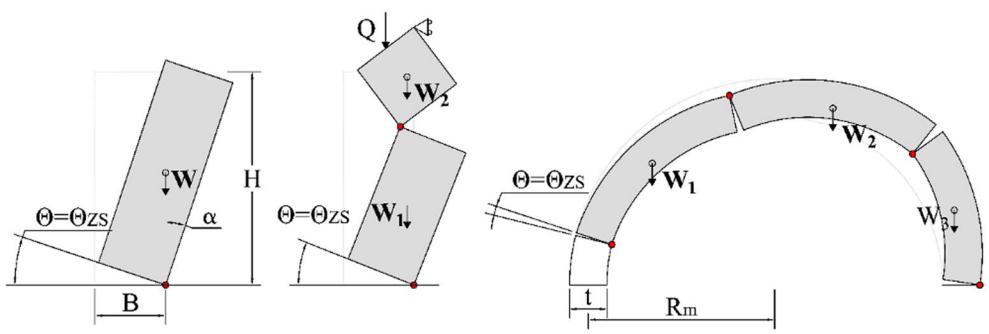

Fig. 8 Configurations of zero strength of the column, of the wall restrained at the head, and of the masonry arch

As an example, Fig. 9 shows the motion of the masonry arch passing from C_{SC} to C_{ZS}. The mechanism of the moving arch is composed by the three segments (C_1- C_{12}), (C_{12}- C_{23}), (C_{23}- C_3), which move and rotate relative to each other around their hinges C_{12} and C_{23} while they change position in the plane of the arch. Consequentially, too the absolute centre C_2 changes position, as shown in Fig. 9, due to the rotation of the segments (C_1- C_{12}), (C_{23}- C_3). The mechanism along which the structure moves, varies its geometry due to the change in position of the hinges C_{12} and C_{23}. The deformation of the arch accumulates, on the other hand, under the pulse sequence and, consequentially, the hinges of the mechanism $\mathbf{u}_0$ will increase monotonically their rotation during the motion from C_{SC} to C_{ZS}.

Appling the principle of virtual work in the deformed configuration:

$$< \mathbf{w}, \delta\mathbf{u}(\boldsymbol{\theta}) > + \lambda(\boldsymbol{\theta}) < \mathbf{f}, \delta\mathbf{u}(\boldsymbol{\theta}) >= 0 \tag{7}$$

the pushover curves (static force or multiplier of the horizontal weight-displacement or rotation relationship) can be found. In these curves the point related to the configuration of zero strength coincides with the intersection of the curve with the abscissa. The pushover curves and the rotations corresponding to the zero strength are plotted in Fig. 10 for the wall restrained at the base and at the top and in Fig. 11 for a masonry circular arch.

5 Definition of the dynamic collapse

The column, during the progressive accumulation of inclination, can reach that configuration C_{ZS} *of zero strength*, in which, both the weight and the acceleration pulse, push *together* the structure to go beyond

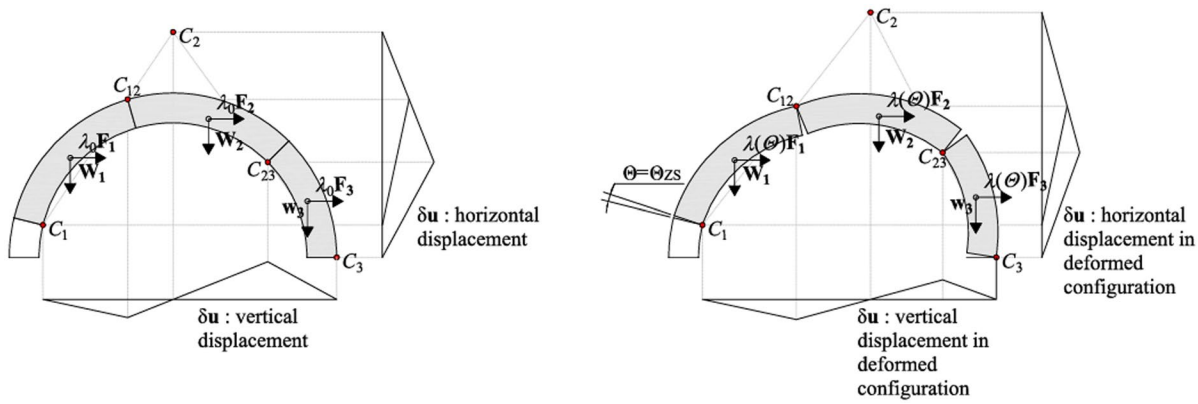

Fig. 9 Changes of configuration of the masonry arch passing from the initial configuration of static collapse to that of zero strength

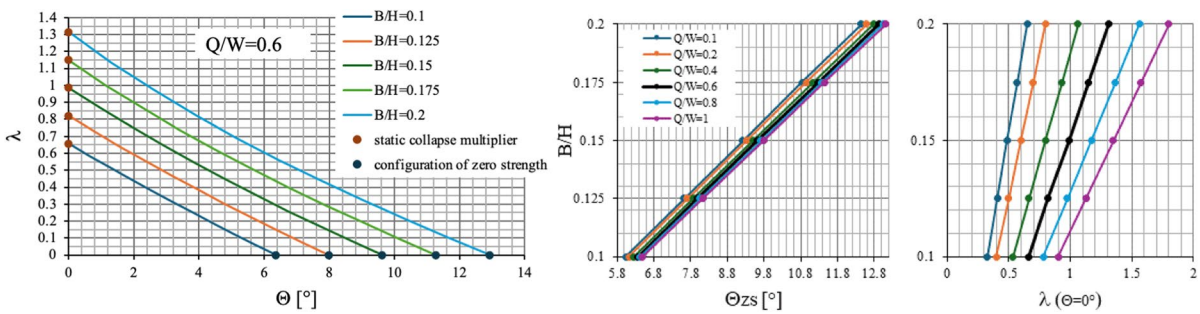

Fig. 10 Pushover curves, limit statical acceleration λ and rotation corrisponding to the configuration of zero strength for masonry wall restrained at the head

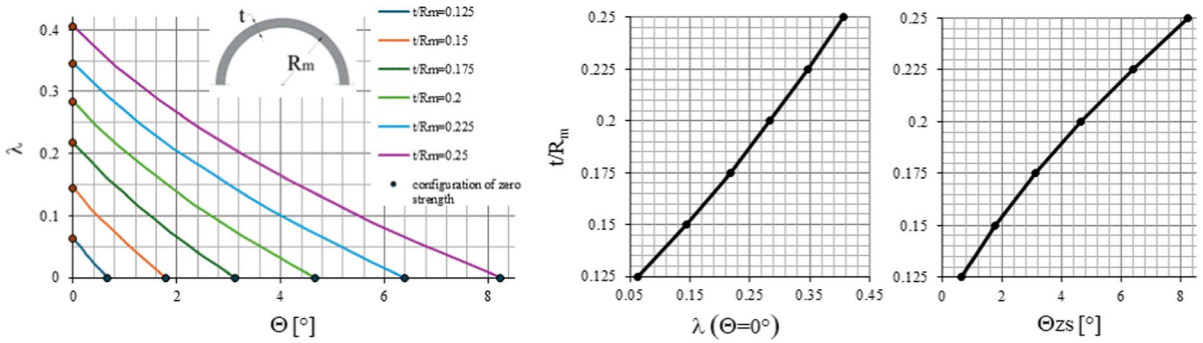

Fig. 11 Pushover curves, limit statical acceleration λ and rotation corrisponding to the configuration of zero strength for masonry circular arches

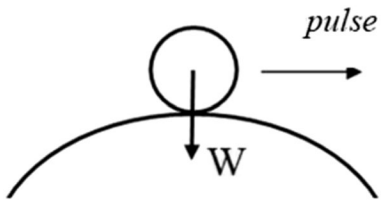

Fig. 12 The idealized collapse state due to the simultaneous occurrence of the zero-strength configuration and the arrival of the pushing action of the acceleration pulse

this configuration (Fig. 12): at this instant the dynamical collapse takes place. This assumption forms the basis of the proposed procedure. Therefore, two requirements are both necessary to reach the collapse for a no tension structure:

1. The reaching the configuration of zero strength θ_{ZS};
2. The simultaneous arrival of the acceleration pulse which pushes the structure to deform further the θ_{ZS}.

Figure 13 shows synthetically the configuration of zero strength reached by the structure at the instant in which the acceleration pulse begins to push,. i.e. the instant in which the dynamical collapse takes place. The attainment of the dynamical collapse in the masonry structure is generally accompanied by the masonry breakdown. In the case of the solid column the dynamical failure occurs because the column, at this point free and without any strength, bounces on the ground.

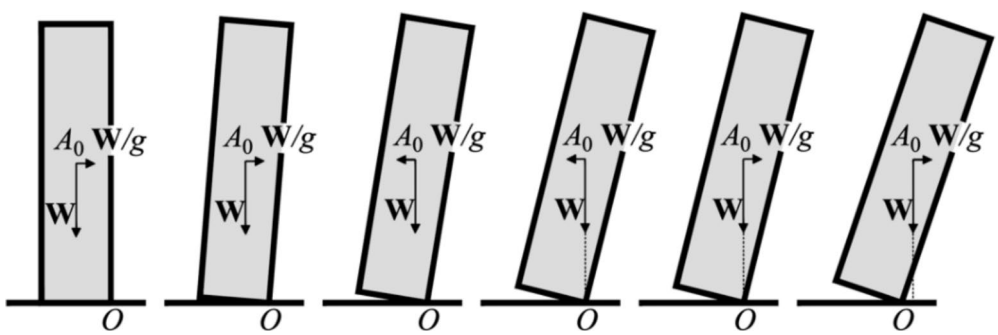

Fig. 13 The collapse of the column occurring at the reaching of the θ_{ZS} configuration

6 The rotation accumulation during the motion of the column hit by pulse sequence

The first analysed case is the masonry column hit by the three sequence S_{03} of rectangular pulses (Fig. 14).

Following the Housner [3] formulation, the equation of the motion of the column, rotating of the angle $\theta_I(t)$ around the base corner, is:

$$\ddot{\theta}_I - p^2\theta_I = p^2\theta_{ZS}\left(q_{03} - 1\right) \tag{8}$$

with the acceleration ratio q_{03}, i.e. the ratio between the dynamical A_{03} and the limit statical A_L accelerations:

$$q_{03} = \frac{A_{03}}{A_L} \tag{9}$$

the pulsation p of the motion and the moment of inertia I_0 of the prismatic column with respect to its base corner:

$$p = \sqrt{\frac{WR}{I_0}}I_0 = \frac{1}{3}\frac{W}{g}4H^2\left(1 + (\tan\alpha)^2\right) \tag{10}$$

where *R is the distance between the centre of gravity and the* base corner, H is the height of the column and α the slenderness.

The same Eq. (8) describes the motion of any no-tension structure if we place in it the corresponding effective pulsation p and the rotation θ_{ZS} of zero strength, both obtained by an appropriate analysis [13, 14].

Solution of (8), with the initial conditions regarding the rotation and angular velocity at time $t=0$, both equal to zero, is:

$$\theta_I(t) = \theta_{ZS}\left(q_{03} - 1\right)(\cosh pt - 1) \tag{11}$$

so that the rotation and the rotation velocity of the column at the end of the first pulse are respectively

$$\begin{aligned}\theta_I\left(t_0\right) &= \theta_{ZS}\left(q_{03} - 1\right)\left(\cosh pt_{03} - 1\right)\dot{\theta}_I\left(t_0\right)\\ &= \theta_{ZS}\left(q_{03} - 1\right)p\left(\sinh pt_0\right)\end{aligned} \tag{12}$$

We note from (11) that the rotation $\theta_I(t_0)$ of the column at the end of the first pulse increases by increasing both as the acceleration ratio q_{03} as the pulse duration t_0.

Assume now that, at the end of the first pulse, the rotation $\theta_I(t)$ has not yet reached the critical value θ_{ZS} so that:

$$\theta_I\left(t_0\right) = \theta_{ZS}\left(q_{03} - 1\right)\left(\cosh pt_0 - 1\right) < \theta_{ZS} \tag{13}$$

When $t > t_0$ the column is stroked by the second pulse and the equation of the motion of the column becomes:

$$\ddot{\theta}_{II} - p^2\theta_{II} = -p^2\theta_{ZS}\left(q_{03} + 1\right) \tag{14}$$

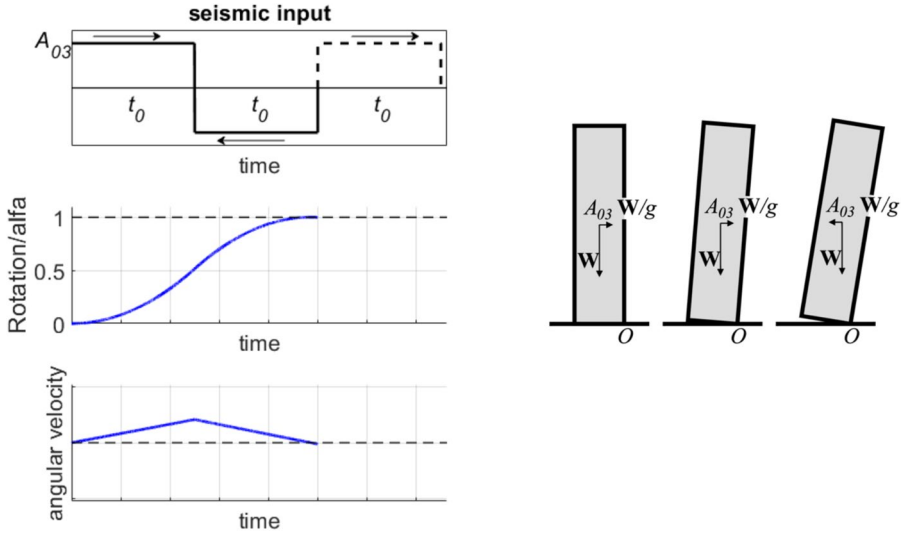

Fig. 14 The three pulse sequence and the rotation/a and angular velocity of the masonry column and the accummulation of inclination in the column

The function $\theta_{II}(t\text{-}t_0)$ is connected to the rotation function $\theta_I(t)$ of the first motion by means the conditions

$$\theta_{II}(t_0) = \theta_I(t_0)\dot{\theta}_{II}(t_0) = \dot{\theta}_I(t_0) \tag{15}$$

By integration of Eq. (13) and considering the Eq. (14), the second motion turns out to be defined by the function:

$$\theta_{II}(t) = \frac{\dot{\theta}_I(t_0)}{p}\sinh\left(p(t-t_0)\right) + \theta_{ZS}(q_{03}+1\left[\theta_I(t_0) - \theta_{ZS}(q_{03}+1)\right]\cosh\left(p(t-t_0)\right)) \tag{16}$$

The ratio between the rotations, respectively evaluated at the ends of the second and of the first pulses, considering the Eq. (12) and the Eq. (15) and that the rotation at the end of the second pulse for hypothesis is equal to θ_{ZS}, is

$$\psi = \frac{\theta_{II}(2t_0)}{\theta_I(t_0)} = \frac{1}{(q_{03}-1)(\cosh pt_{03}-1)} > 1 \tag{17}$$

Therefore, during the action of the second pulse the rotation of the column *continues to grow* even if the second pulse acts in the opposite direction to the first, as consequence of the rotation velocity of the column acquired at the end of the first pulse (Fig. 14).

Considering sequences with a larger number of pulses, in spite that the acceleration pulses follow one after the other alternatively, the inclination continues to grow (Fig. 13).

Remark There is a deep link between the *static* theory of no tension structures and the theory of Plasticity. Similarly, there is an analogy between the incremental collapse and the shakedown occurring in Plasticity and the dynamical response of no tension structures under sequences of alternating acceleration pulses, marked by the develpment, as above shown, of accumulation of deformations under the repeated action of alternating pulses of the sequence.

7 Confirm of the deformation accumulation by numerical and experimental investigations

Figure 15 shows the rotation of a rigid masonry wall (with $H=4$ m and $\alpha=0.1$) until collapse is achieved by scaling two real accelerograms (in the emotion equation: $\ddot{u}_g(t)$). For these seismic inputs, the numerical integration of the motion equation:

$$\ddot{\theta}_I - p^2\theta_I = p^2\ddot{u}_g(t) \tag{18}$$

is performed with ODE45 solver in MATLAB® [18].

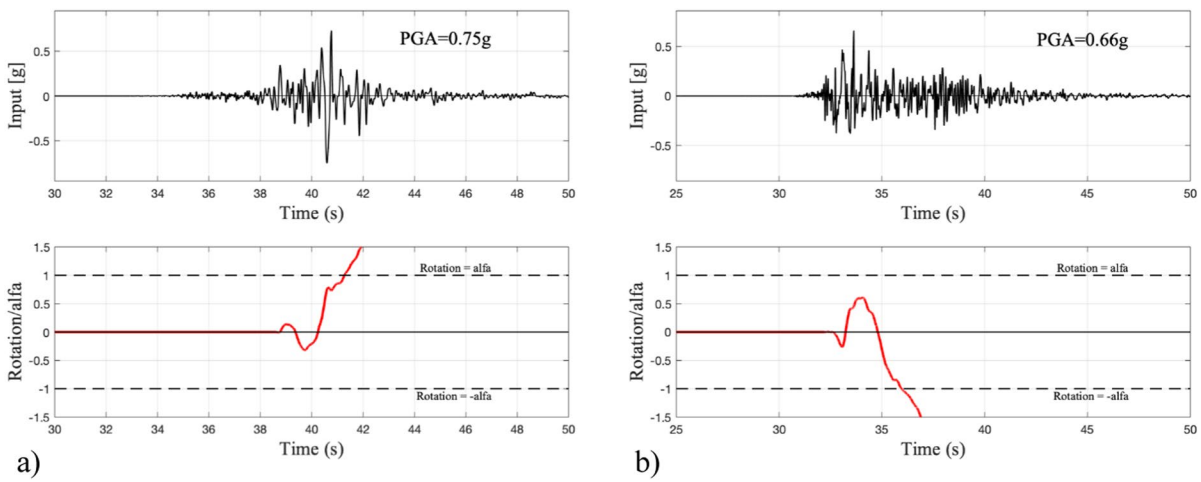

Fig. 15 Accumulation of the rotation of the masonry wall: scaled real accelerogram: **a** central Italy 30/10/2016 station MZ51; **b** L'Aquila 06/04/2009 station AQV (from: Felicetta et al. [17])

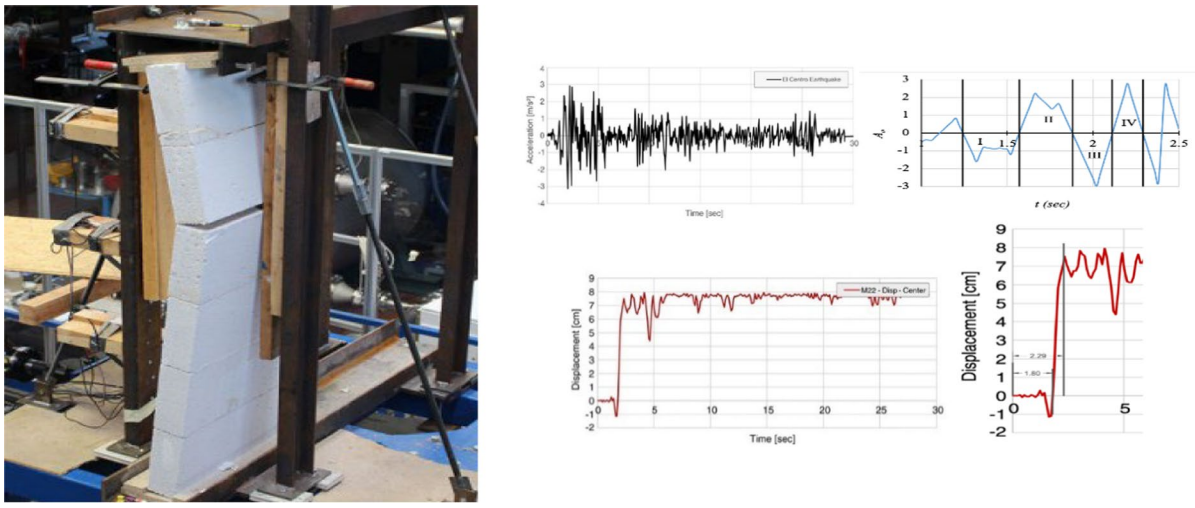

Fig. 16 Test set up and obtained results from Lönhoff and Sadegh-Azar [18]

The obtained results confirm the central result of the above theoretical research: the accumulation of rotation under alternative pulses. During the ascending branch, while the acceleration pulses follow one after the other alternatively, the rotation of the column increases more or less uniformly.

In the test performed by Lönhoff and Sadegh-Azar [19] the time history of the El Centro Earthquake was used, with peak accelerations of 3.14 m/s^2 reached after 2 s (Fig. 16). During the ascending branch, while the acceleration pulses follow one after the other alternatively, the displacement of the wall increases constantely. As the diagram shows, the collapse occurs with the appearance of a sudden uniform accumulation of deformation of the wall, without showing any, even small, inversion of sign, despite the alternating nature of the violent shocks.

8 Research of the collapse sequences. The limit collapse sequence S_{03}

A three-pulse sequence is a *limit collapse sequence* S_{03} if the intensity of the pulses and their duration are such that to bring the column into the θ_{ZS} configuration just at the end of the second pulse. The arrival of the third pulse, pushing the column to go beyond the θ_{ZS} produces the collapse.

The limit collapse sequence is characterized by the critical limit acceleration ratio q_{03}, corresponding to the chosen duration pt_0, able to assure that at the end of the second pulse the structure reaches the zero strength configuration, i.e. such that:

$$\theta_{II}(2t_0) = \theta_{ZS} \tag{19}$$

Solution of (19) gives *the corresponding critical limit collapse acceleration ratio:*

$$q_{03} = \frac{A_0}{A_L} = \frac{2\left(\cosh(pt_0)\right)^2 - 1}{2\cosh(pt_0)\left(\cosh(pt_0) - 1\right)} \tag{20}$$

By varying the specific pulse duration pt_0 the Eq. (20) traces the C_{03} curve, i,e, *the limit collapse acceleration curve* representative of the $q_{03}(pt_0)$ function [12] (Fig. 17):

$$C_{03} = \left[pt_0 > 0, q_{03}(pt_0)\right] \tag{21}$$

9 Generation of collapse sequences by gradually changing the acceleration ratio q

9.1 Three pulse critical sequences with acceleration ratio, or pulse duration, larger than q_{03} or pt_0

In the place of the collapse sequence S_{03}, let us consider any three-pulses sequence S'_3 having

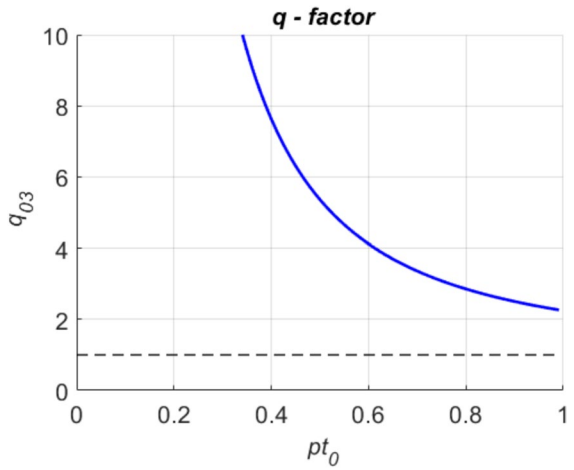

Fig. 17 The *limit collapse acceleration curve* C_{03}

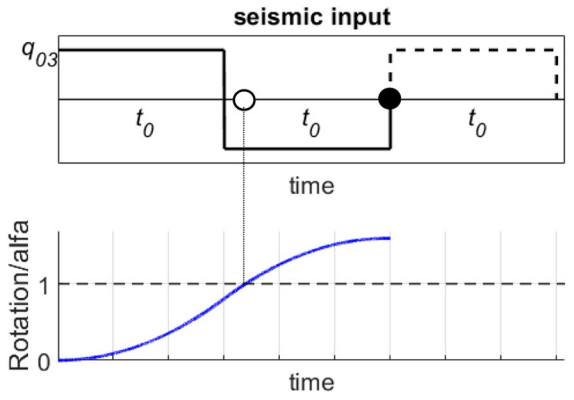

Fig. 18 The instant of the attainment of the $\theta_{ZS}(=\alpha)$, (white dot), that prevents the reaching of the collapse (black dot)

$q'_{03} > q_{03}$; the column, hit by this sequence, acquires greater rotation speed and will reach the θ_{ZS} before the end of the second pulse. On the other hand, as the pulse continues to act, the rotation of the column further increases, and the collapse occurs again at the beginning of the third pulse. Figure 18 shows the instant of the attainment of the $\theta_{ZS,}$ defined by the white dot, that prevents the reaching of the collapse, defined by the black dot (Fig. 18).

Consequentially, the limit collapse ratio $q_{03} = A_{03}/A_L$, defined by (20), is the smallest acceleration ratio, among all the critical ratios $q'_{03} = A'_{03}/A_L > q_{03}$ of the collapse three pulse sequences having pulses with duration pt_0.

9.2 Collapse three pulse sequences with acceleration ratio, or pulse duration, lower that q_{03} or pt_0

The rotation of the column decreases if q_{03} decreases so that, under any three-pulse sequence S'_3, with $q'_{03} < q_{03}$, the column, rotating more slowly, cannot reach the θ_{ZS} at the end of the second pulse (Fig. 19) as occurs when the column is struck by the sequence S_{03}. The situation is similar if we consider acting on the column, or on the no tension structure, the three pulse sequence S''_{03} with the pulse duration $pt''_3 < pt_0$. Even in this case the column cannot reach the θ_{ZS} at the end of the second pulse, but later, and the collapse takes places as soon as the θ_{ZS} is reached during the third pulse.

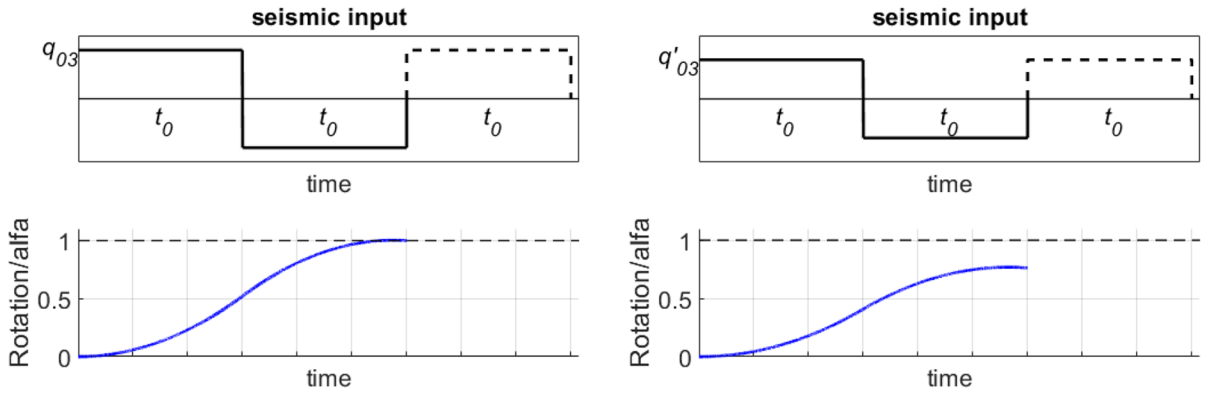

Fig. 19 The limit collapse three pulse sequence S_{03} and the three pulse sequence S'_{03} ($q'_{03} < q_{03}$)

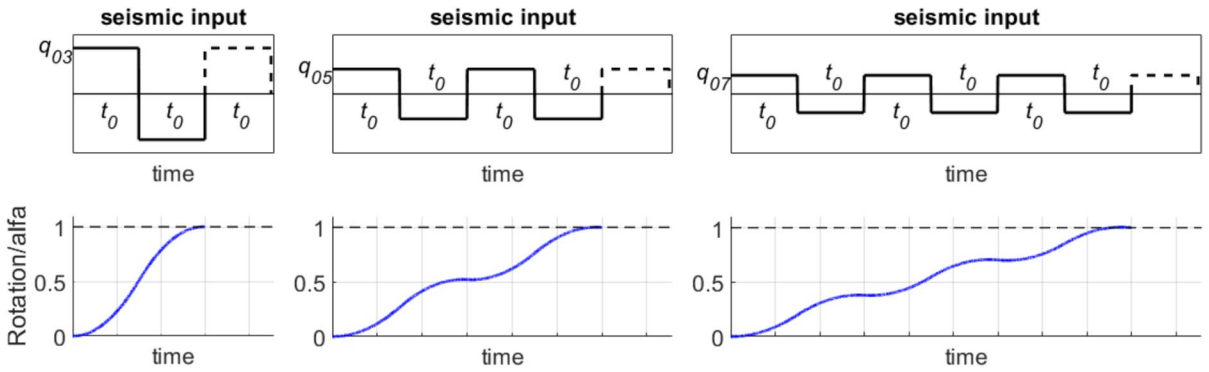

Fig. 20 The limit collapse sequences q_{03}, q_{05}, q_{07}

10 Limit collapse acceleration sequences with an increasing number of pulses

In a limit collapse sequence the θ_{ZS} is reached at the penultimate pulse so that the succeeding pulse pushes the column to rotate beyond θ_{ZS}. The collapse takes place. Figure 20 shows the chain of the limit critical sequences of pulse accelerations: they present a number of pulses gradually increasingwhen the corresponding acceleration ratios are reduced.

For any chosen value of the pulse duration pt_0 the corresponding limit collapse acceleration ratios q_{0N} of pulse sequences therefore decrease by increasing the pulse number N of the sequences so that

$$q_{03}(pt_0) > q_{05}(pt_0) > q_{07}(pt_0) > \dots \tag{22}$$

The limit collapse acceleration ratios q_{0N} become gradually smaller and closer to each other. They contract on an asymptotic value q that is their minimum. At the same time, due to the concentration of the q_{0N} near q, it is close to the mean value of the q_{0N}. The corresponding C_{03}, C_{05} and C_{07} curves follow the same behaviour and converge on an asymptotic curve (Fig. 21).

Following the results of a numerical investigation, it turns out that this asymptotic curve can be well represented by the curve C_{07} [14] defined as:

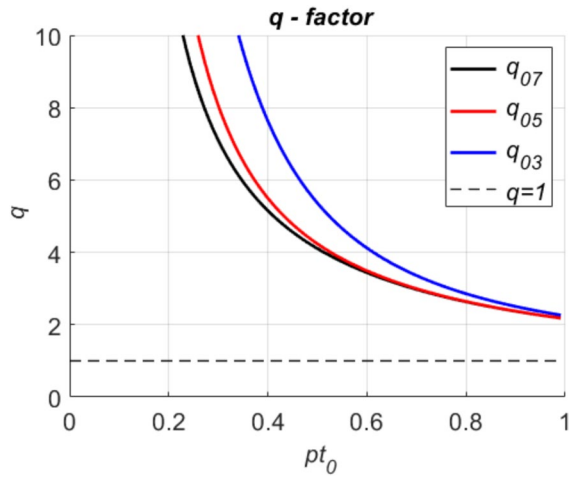

Fig. 21 Obtaneid q-factor versus pt_0

11 The seismic design

The seismic design evaluates the real resistance capacity of the structure with the resistance required to withstand the expected earthquake. The common seismic design is based on two quantities that identify the expected earthquake: the *PGA*, i.e. the maximum horizontal peak ground acceleration, and the period T_E.

The resistant capacity of the structure is here verified

$$q(pt_0) \approx q_{07}(pt_0) = \frac{\cosh(6pt_0)}{2\cosh(pt_0)\left(2\cosh(4pt_0)+1\right)\left(\cosh(pt_0)-1\right)} \tag{23}$$

with respect to the action of a long sequence of pulses,

to which corresponds the minimum value of the limit collapse acceleration ratio q, evaluated considering the long sequence of pulses ($N=7$) (Fig. 21).

We take as a basis the asymptotic curve C_{07} relating to the asymptotic sequence S_{07} with a large number of pulses (Fig. 21). The acceleration ratio q_{07} is known and is given by (23).

The dynamical acceleration A_0 of pulses of the sequence S_0, is assumed equal to the expected acceleration *PGA*. The limit static acceleration A_{L_REQ} required so that the structure can sustain the expected earthquake is:

$$A_{L\_REQ} = \frac{PGA}{q_0^*} \tag{24}$$

where the value of $q(pT_E/2)$ is detected by the diagrams of Fig. 21 or is given by:

$$q(pt_0) \approx q_{07}(pt_0) = \frac{\cosh(6pT_E/2)}{2\cosh(pT_E/2)\left(2\cosh(4pT_E/2)+1\right)\left(\cosh(pT_E/2)-1\right)} \tag{25}$$

More explicitly, the (24), using (25) is

$$A_{L\_REQ} = PGA\frac{2\cosh(pT_E/2)\left(2\cosh(4pT_E/2)+1\right)\left(\cosh(pT_E/2)-1\right)}{\cosh(6pT_E/2)} \tag{26}$$

The real static limit acceleration A_{L_REAL} (αg for the simple masonry wall, and the value reported in Figs. 10 and 11 multiplied by g for the masonry wall restrained at the top and for the circular masonry arches, respectively) necessary to protect the structure by the considered sequence of seismic pulses has therefore to satisfy the condition

$$A_{L\_REAL} \geq PGA\frac{2\cosh(pT_E/2)\left(2\cosh(4pT_E/2)+1\right)\left(\cosh(pT_E/2)-1\right)}{\cosh(6pT_E/2)} \tag{27}$$

We observe that if, instead of assuming the C_{07} curve, we had considered, for instance, the C_{05} curve, the corresponding q_{05} ratio that is $q_{05}>q$ would have determined the corresponding limit static acceleration *required*:

$$\frac{PGA}{q_{05}} < A_{L\_REQ} \tag{28}$$

and, consequentially, an *unsafe* condition compared to (27).

The assumption of the acceleration ratio q as the basis in the seismic design which is the minimum among all the acceleration ratio q_{0N}, guarantees the full safety in the seismic design.

12 Conclusions

The paper highlights the inadequacy of the models commonly used in the seismic design of masonry structures. These models, unlike those used for reinforced concrete or steel structures, are in fact based on the use of the elastic plastic oscillator, which takes into account their capacity to dissipate energy by means of ductility. On the contrary, masonry structures, whose behavior is founded on the no-tension Heyman model, don't exhibit in any way elastic behavior and don't even present an oscillation period. The paper has therefore developed a new dynamical collapse analysis of masonry structures affected by sequences of simple pulses of horizontal acceleration. The paper points out the two new aspects that play a fundamental role in defining the dynamical collapse of the masonry structures: the critical, or the zero-strength configuration, that the structure has to reach just before the collapse, and the accumulation of deformation that takes place in the structure if hit by sequences of horizontal acceleration pulses, alternating in sign. Collapse thus takes place under the simultaneous achievement of the configuration of zero-strength θzs and the arrival of the subsequent acceleration pulse that pushes the structure to go beyond the θzs. The collapse of the

structure is ruled by the limit critical acceleration ratio q (i.e. the so-called force reduction factor) between the magnitude of the limit collapse horizontal acceleration A_0 and the static limit acceleration A_L of the structure: it depends on the number of pulses and on their wave length pt_0, dilated or contracted compared to the real pulse duration t_0, by means the pulsation p of the motion of the structure.

By increasing the pulse number N, the limit collapse acceleration ratios q_{0N} become gradually smaller and closer to each other. They contract on an asymptotic value q—the minimum among all the limit collapse sequences of any order N—that is considered the basis of the corresponding procedure, proposed in the paper, of the seismic design.

Author contribution Simona Coccia and Mario Como wrote the main manuscript text and Simona Coccia prepared figures. All authors reviewed the manuscript.

Funding Open access funding provided by Università degli Studi di Roma Tor Vergata within the CRUI-CARE Agreement.

Data availability No datasets were generated or analysed during the current study.

Declarations

Conflict of interests The authors declare no competing interests.

References

1. Hussain N (2024) Seismic response factors of code-designed high-rise buildings using 3D non-linear analysis (Doctoral dissertation, University of British Columbia)
2. Circolare 2 febbraio 2009 n. 617 C.S.LL.PP. Istruzioni per l'applicazione delle nuove norme tecniche per le costruzioni di cui al decreto ministeriale 14 gennaio 2008. Supplemento ordinario n. 27 alla Gazzetta Ufficiale 26 febbraio 2009, 47, 229–392
3. Housner GW (1963) The behavior of inverted pendulum structures during earthquakes. Bull Seismol Soc Am 53(2):403–417
4. Sorrentino L, Alshawa O, Decanini LD (2011) The relevance of energy damping in unreinforced masonry rocking mechanisms. Experimental and analytic investigations. Bull Earthq Eng 9:1617–1642
5. Bisegna P, Coccia S, Como M, Nodargi NA (2023) A novel impact model for the rocking motion of masonry arches. Meccanica 58(10):2079–2093
6. Como M, Di Carlo F, Coccia S (2019) Dynamic response of rocking cracked masonry walls. Meccanica 54:381–398
7. Coccia S, Di Carlo F, Imperatore S (2017) Force reduction factor for out-of-plane simple mechanisms of masonry structures. Bull Earthq Eng 15:1241–1259
8. DestroBisol G, Prajapati S, Sorrentino L, AlShawa O (2024) Vertical spanning wall elastically restrained at the top: validation and parametric dynamic analysis. Bull Earthq Eng 22(8):3951–3978
9. Giresini L, Solarino F, AlShawa O (2025) Dissipative tie-rods restraining one-sided rocking masonry walls: analytical formulation and experimental tests. Bull Earthq Eng 23(2):779–804
10. Makris N, Vassiliou MF (2013) Planar rocking response and stability analysis of an array of free-standing columns capped with a freely supported rigid beam. Earthquake Eng Struct Dynam 42(3):431–449
11. Voyagaki E, Psycharis IN, Mylonakis G (2013) Rocking response and overturning criteria for free standing rigid blocks to single—lobe pulses. Soil Dyn Earthq Eng 46:85–95
12. Coccia S, Como M, Di Carlo F (2022) The slender rigid block: archetype for the seismic analysis of masonry structures. J Earthq Eng 27(10):2630–2654
13. Coccia S, Como M (2023) Out-of-plane dynamical strength of masonry walls under seismic actions. J Earthq Eng 28(4):1040–1068
14. Coccia S, Como M (2024) Dynamical collapse of masonry arches under sequences of impulses of horizontal acceleration. J Earthq Eng 28(16):4644–4671
15. Heyman J (1966) The stone skeleton. Int J Solids Struct 2(2):249–279
16. Como M (2013) Statics of historic masonry constructions, vol 1. Springer, Berlin
17. Felicetta C, Russo E, D Amico M, Sgobba S, Lanzano G, Mascandola C, Pacor F, Luzi L (2023) Italian Accelerometric Archive v 4.0—Istituto Nazionale di Geofisica e Vulcanologia, Dipartimento della Protezione Civile Nazionale. https://doi.org/10.13127/itaca.4.0
18. Matlab S (2012) Matlab. The MathWorks, Natick, MA, 9
19 Lönhoff M, Sadegh-Azar H (2018) Seismic out-of-plane behavior of unreinforced masonry walls. ce/papers 2(4):291–299